Dear author,

Please note that changes made in the online proofing system will be added to the article before publication but are not reflected in this PDF.

We also ask that this file not be used for submitting corrections.

Mechanical Systems and Signal Processing xxx (xxxx) xxx

Contents lists available at ScienceDirect

Mechanical Systems and Signal Processing

journal homepage: www.elsevier.com/locate/ymssp

FP+DIC for low-cost 3D full-field experimental modal analysis in industrial components

Luis Felipe-Sesé [a], Ángel J. Molina-Viedma [b,*], Elías López-Alba [b], Francisco A. Díaz [b,1]

[a] Departamento de Ingeniería Mecánica y Minera, Campus Científico Tecnológico de Linares, Universidad de Jaén, 23700 Linares, Spain
[b] Departamento de Ingeniería Mecánica y Minera, Campus Las Lagunillas, Universidad de Jaén, 23071 Jaén, Spain

ARTICLE INFO

Article history:
Received 26 November 2018
Received in revised form 26 February 2019
Accepted 7 April 2019
Available online xxxx

Keywords:
Fringe Projection
Digital Image Correlation
3D modal characterisation

ABSTRACT

High Speed 3D Digital Image Correlation has reached notorious popularity in dynamic characterisations because of the full-field non-invasive performance. It is being especially relevant for experimental modal analysis due to the importance of the modal parameters to define the dynamic behaviour. However, the economic cost of a stereoscopic system of two high speed cameras is a main concern regarding traditional instrumentations. In the search for low-cost alternatives, different methodologies have arisen that employ a single camera for 3D measurements. One approach consists in obtaining a stereo-vision in a single image using, for instance, a mirror system. These approaches involve important field-of-view restrictions. An interesting approach employs the full resolution by combining Fringe Projection and 2D-DIC for out-of-plane and in-plane displacements, respectively. In this study, this technique is explored to perform experimental modal analysis in a large non-flat aeronautical panel. The validation of the results has been performed using accelerometer measurements during an impact hammer test. The results of the study stand this technique as an attractive low-cost technique for 3D full-field modal characterisations of complex components.

1. Introduction

Full-field experimental modal analysis is a new trend thanks to new advances and studies in full-field optical techniques supported by the development of the high speed cameras technology that makes it possible the high-definition images capture at high frame rates [1]. This popularity is based on a considerable improvement to perform experimental modal analysis provided by non-invasive full-field measurements. Traditional instrumentations face some uncertainties in the measurement such as natural frequencies and damping perturbation due to the transducers mass and cabling effect [2,3]. Additionally, they perform pointwise measurements and hence only a limited number of points are measured from the whole structure. That could be an important limitation for large components even yielding spatial aliasing. Moreover, the full-field information provided by this technique is an essential tool in the validation and improvement of both theoretical and numerical models. Nevertheless, these are considerably less sensitive and the equipment usually more expensive [4–6].

Among these full-field techniques, High Speed 3D Digital Image Correlation (HS 3D-DIC) outstands. 3D-DIC is a reliable technique and widespread in experimental mechanics that is able to perform 3D displacement measurements with a simple

* Corresponding author.
E-mail address: ajmolina@ujaen.es (Á.J. Molina-Viedma).
[1] ORCID: 0000-0003-0467-542X.

https://doi.org/10.1016/j.ymssp.2019.04.004
0888-3270/

setup as a main advantage [7]. Many studies have demonstrated the capabilities of HS 3D-DIC to characterise full-field mode shapes or operational deflection shapes in beam or plate-like objects [4,5,8–11] as well as industrial applications like turbine blades [12] or aerospace components under inflight conditions [13]. Nevertheless, different studies went further and addressed complete modal characterisations [6,14–16] using established modal identification algorithms in full-field Frequency Response Functions (FRF). Some of them performed this modal identification in real mechanical systems like artificial beetle's wing for micro air vehicles [17] and automobile components like a car bonnet [18] or a multicomponent lighting system [19].

However, the economic cost of a stereoscopic system, especially when high speed cameras are required, such is for modal analysis, motivated that different alternatives to 3D-DIC have been explored in the last years. In fact, two main alternatives have been presented which employ a single camera for 3D measurements. The first one relies on optical methodologies to obtain two images from a single capture of the camera [20], i.e., diffraction grating [21], prim-based [22] or mirror-based [23]. In such cases, image obtained by a single camera was divided into two images, in each of them it is observed the region of interest from two different points of view in order to have a stereoscopic optical system. Thus, the optical system could be calibrated using standard methods and images processed employing 3D-DIC algorithms. An important common disadvantage is the requirement of dividing the image of the camera in two different images, which could be an important issue for large components. Yu and Pan [24] addressed a first approach to modal analysis on a flat plate using a mirror-based single-camera stereo-DIC system. The peak-picking procedure was employed to identify the natural frequencies and the half-power method for the damping ratio on the fast Fourier transform of the measurement instead of FRFs. Then, operational deflection shapes were obtained measuring the response to single resonances during additional tests.

A second approach is the integration of two-dimensional digital image correlation (2D-DIC) to measure in-plane displacements and Fringe Projection (FP) for shape and out-of-plane displacements (FP+DIC). This approach, unlike previous one, employs the whole field of view of a camera. The fundamentals were investigated by previous researchers [25–32] and authors of this work recently proposed a more flexible integration methodology to measure 3D shape and displacements in solids [33,34]. Hence, is possible to measure simultaneously in-plane (Δx, Δy with 2D-DIC) and out-of-plane displacements or shape (Δz with FP) using only one camera and an additional fringe projector. The method employs a single sensor camera (CCD or CMOS) with conventional lenses and a post-processing correction of the in-plane distortion resulting from the out-of-plane displacements or shape of the specimen. FP requires a clear fringe pattern to operate adequately and DIC requires a speckle pattern. Due to the dynamic nature of vibration testing, both patterns should represent the same instant time and, hence, each image should include both speckle and fringe pattern. To make this possible without mutually interfering both patterns, colour encoding by employing RGB camera is employed [31,35]. The result is a simple 3D displacement measurement system with a spatial resolution comparable to commercial 3D-DIC. Actually, this methodology has been successfully applied to different static or dynamic tests of different size of specimens [33,36,37]. Nonetheless, previous vibration analyses were simply focus on harmonic excitation for ODSs measurement and no complete modal characterisation was performed.

Therefore, considering the benefits of the combination of FP+DIC, this work proposes the technique for experimental modal analysis as a low-cost alternative to 3D-DIC. A large industrial component was employed for the determination of full-field FRFs. This component is a non-flat large composite panel (roughly 3 m^2) from aeronautic industry, pushing the technique toward real, practical applications. Modal parameters were inferred from the full-field FRFs using the circle-fit approach [2]. Results were satisfactorily validated with those obtained from a well-established procedure which is the impact hammer testing. From the comparison, the benefits of 3D full-field modal analysis were also exposed.

2. FP+DIC fundamentals

A main incentive of this study is the determination of full-field 3D displacement information with just a single high speed camera. For that purpose, a combination of FP [38] and 2D-DIC [39] has been employed based on earlier work [33,34].

Fringe projection relies on obliquely projecting parallel fringes on the specimen surface to measure its out-of-plane displacement. This fringe pattern exhibits deformation when the specimen experiences shape changes in the optical axis direction. According to this, the images of a flat reference plane and the specimen during deformation are analysed to extract a continuous map of out-of-plane displacements or shape. On the other hand, 2D-DIC is a full-field optical technique employed to measure displacements in the sensor plane [40]. This technique is light-intensity-based and relying on the use of digital image processing. In this technique, areas of recorded images are grouped into virtual sets of pixels called facets which are tracked in subsequent images when displacement occurs. To perform a proper tracking, specimen surface should present a randomly distributed speckle pattern to guarantee the singularity of each facet.

The integration of FP and 2D-DIC employs a conventional colour LCD projector and a colour RGB high-speed camera. The projector is used to create a blue fringe pattern on white background with a sinusoidal intensity profile on the measured surface. That permits fringe projection analysis to be performed in the blue spectrum of the recorded images to achieve out-of-plane displacements (Z direction) [25,31]. In addition, a red speckle pattern on a white background is painted onto the measured surface to permit 2D-DIC [39] to be performed in the red spectrum and measure in-plane displacements (X and Y directions).

Please cite this article as: L. Felipe-Sesé, Á.J. Molina-Viedma, E. López-Alba et al., FP+DIC for low-cost 3D full-field experimental modal analysis in industrial components, Mechanical Systems and Signal Processing, https://doi.org/10.1016/j.ymssp.2019.04.004

The combination takes into account that the in-plane displacements from 2D-DIC are affected by distortion due to the out-of-plane displacement of the specimen when a telecentric lens is not employed [25,33]. The distortion is corrected using the out-of-plane displacements measured by FP with a methodology based on a pin-hole model of lenses [33] according to Eq. (1) and Fig. 1:

$$\begin{cases} \Delta x = L\left[\Delta x_{CCD} - \left(x_{2,CCD}\frac{\Delta z_2}{z_0} - x_{1,CCD}\frac{\Delta z_1}{z_0}\right)\right] \\ \Delta y = L\left[\Delta y_{CCD} - \left(y_{2,CCD}\frac{\Delta z_2}{z_0} - y_{1,CCD}\frac{\Delta z_1}{z_0}\right)\right] \end{cases} \quad (1)$$

where $(x_{1,CCD}, y_{1,CCD})$ and $(x_{2,CCD}, y_{2,CCD})$ are the initial and final position of a displaced pixel at the element surface, Δz_1 and Δz_2 are the corresponding out-of-plane displacement at corresponding pixel, z_0 is the distance between the reference surface and the optical centre of the camera lens and L is the inverse of the lateral magnification at z_0. These required parameters are estimated by a calibration procedure where the optical axis of the camera is perpendicularly aligned to a flat reference surface [34,41].

3. FP+DIC experimental setup

In this work, the technique was evaluated in a composite panel employed in aerospace industry. The panel was curved and has different bumps caused by stiffeners. Thus, this complex shape contributes to show the potential of FP+DIC as low-cost 3D full-field technique. For the subsequent tests, the panel was hanged in a frame under free-free boundary conditions as observed in Fig. 2(a) together with the optical setup.

As commented, FP+DIC optical system consisted on a high speed camera and a LCD projector. Particularly, a Photron SA3 RGB colour camera was employed with a resolution of 1024 × 1024 pixels and Vivitar 28 mm focal length lens and a Epson W32 projector placed at 1.2 m from the camera. Speckle and fringe patterns were decomposed into different images by RGB encoding [31,42]. As the whole panel surface cannot be visualised due to its shape, the optical arrangement was focus on half the panel with certain angle considering symmetry, as seen in Fig. 2. Calibration of this optical set-up was performed following the methodology previously developed by the authors for big specimens. A smaller panel (rigid flat panel of 1 × 1m) was placed at 3.75 m from optical axis of the camera and at three different positions (left, centre and right) as performed by Felipe-Sesé et al. [36] and employing an automatic calibration procedure also previously developed [41]. This optical arrangement leaded to the optical magnification for the camera of 2.2 mm/pixel and a fringe relation of 8.5 mm/radian. The minimum uncertainty for this set-up was considered of 0.470+/−0.07 mm [36].

The surface of the specimen was painted with white paint and red speckle pattern (of 5–15 pixel size) by employing brushes to provide a suitable pattern for 2D-DIC. The Red data of images, where fringes were observed, were processed using a Fourier Profilometry [43] combined with a quality unwrapping algorithm [44] to obtain 3D-shape map. The Blue data containing speckle images were processed using a commercial digital image correlation algorithm (VIC 2D from Correlated Solutions Inc.) employing a facet of 29 pixels.

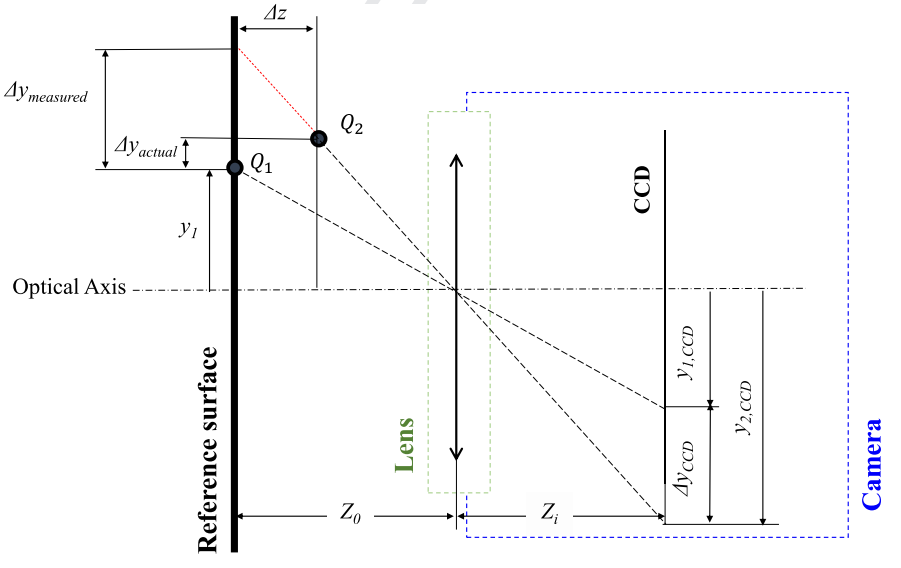

Fig. 1. Pin-hole model lenses showing in-plane displacement error induced in 2D-DIC due to the out-of-plane displacements during a deformation from the Q1 to Q2 position.

Please cite this article as: L. Felipe-Sesé, Á.J. Molina-Viedma, E. López-Alba et al., FP+DIC for low-cost 3D full-field experimental modal analysis in industrial components, Mechanical Systems and Signal Processing, https://doi.org/10.1016/j.ymssp.2019.04.004

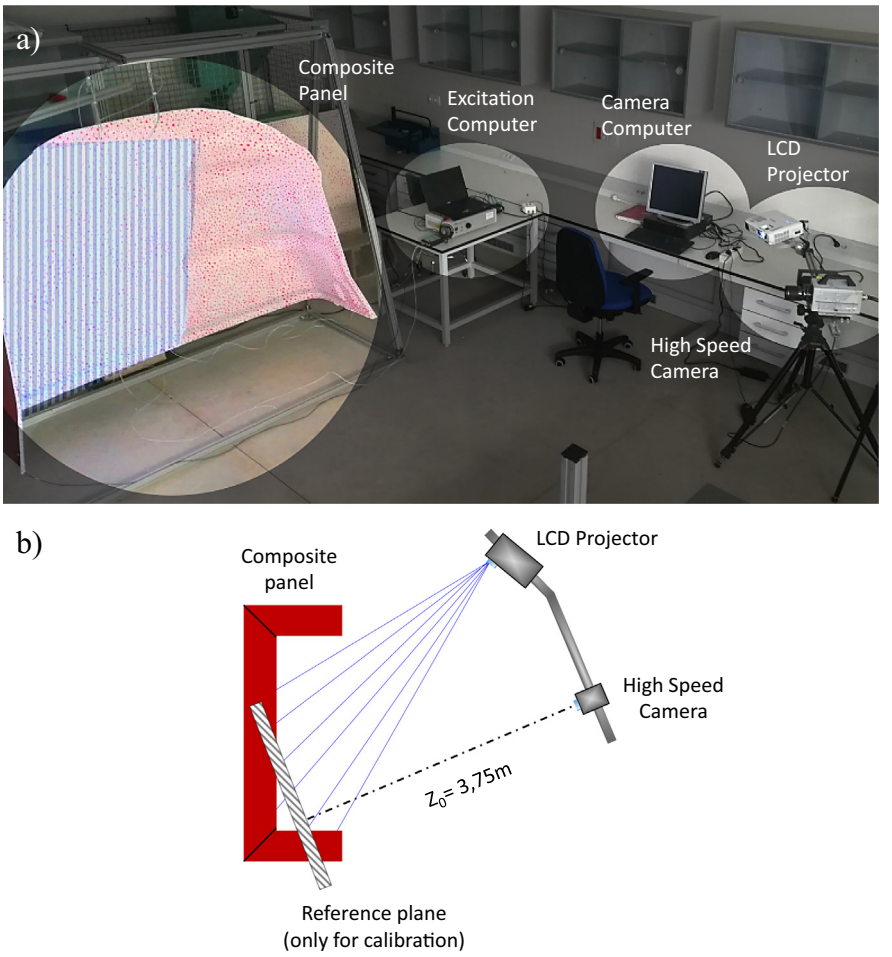

Fig. 2. Optical setup for FP+DIC measurement on the free-free hanged panel. (a) Real picture. (b) Schematic.

For modal identification the spectrum up to 100 Hz was examined exciting the panel using a noise signal. The force was applied through a stinger using an electrodynamic shaker model Data Physics GW-V20/PA30E from behind the panel. The excitation point was located in the middle close to the lower edge as indicated in Fig. 3. A load cell was employed to obtain the force signal.

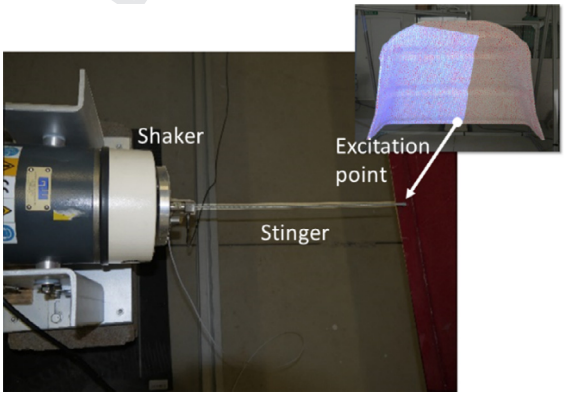

Fig. 3. Excitation configuration employing a shaker provided with stinger.

Please cite this article as: L. Felipe-Sesé, Á.J. Molina-Viedma, E. López-Alba et al., FP+DIC for low-cost 3D full-field experimental modal analysis in industrial components, Mechanical Systems and Signal Processing, https://doi.org/10.1016/j.ymssp.2019.04.004

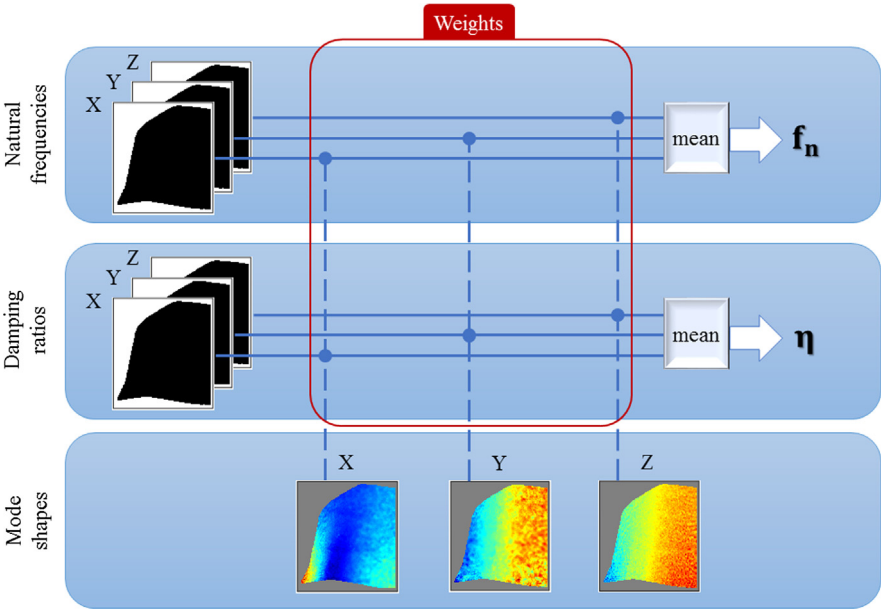

Fig. 4. Modal parameters, i.e., natural frequency, $\mathbf{f_n}$, damping ratio, η, and mode shapes obtained from full-field 3D measurements using FP+DIC and circle-fit approach for one mode.

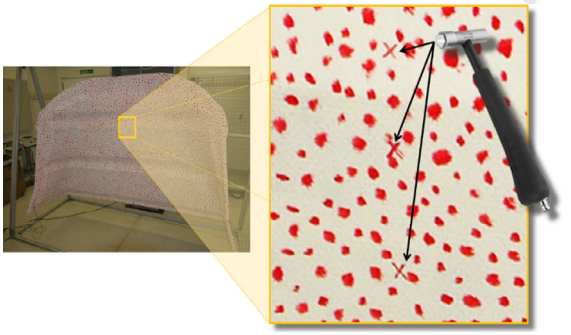

Fig. 5. Drawn crosses in speckle to locate the impact points in the area of interest of FP+DIC.

3.1. Full-field experimental modal analysis

From this test, the response and excitation spectra were analysed to obtain the 3D FRFs of the panel in a full-field manner. For this purpose, both systems were synchronised using a NI USB-6251 DAQ system governed by the camera recording parameters. Namely, 4083 images were recorded during the test with a rate of 250 fps.

The FRFs were obtained by applying the Welch's averaging method [45] to the excitation and response time histories. This processing was performed so that the frequency resolution was 0.33 Hz. The averaging process included 66% windows overlap and hanning windows as anti-leakage method. Considering that 33,335 response points (up to 6 points/cm^2) were measured using FP+DIC, the same number of FRFs were obtained which define the response of each point in the analysed spectrum.

The extraction of natural frequencies, mode shapes and damping ratios was performed for the identified modes in these FRFs using the circle-fit method [2]. This method evaluates the modal parameters by fitting the vicinity of a resonance as a circular geometry as deduced theoretically. As it entails a sequential methodology, it is an efficient method to face the modal identification with such a full-field technique [16,19]. As a result of employing this method for each mode, a set of the three modal parameters (natural frequency, damping ratio and mode shape amplitude) was obtained for each spatial point of the full-field matrix. Additionally, since the 3D behaviour is inspected, three sets corresponding to each displacement direction were obtained for every modal parameter. The extracted data can be reorganised as spatial matrices for each modal param-

Please cite this article as: L. Felipe-Sesé, Á.J. Molina-Viedma, E. López-Alba et al., FP+DIC for low-cost 3D full-field experimental modal analysis in industrial components, Mechanical Systems and Signal Processing, https://doi.org/10.1016/j.ymssp.2019.04.004

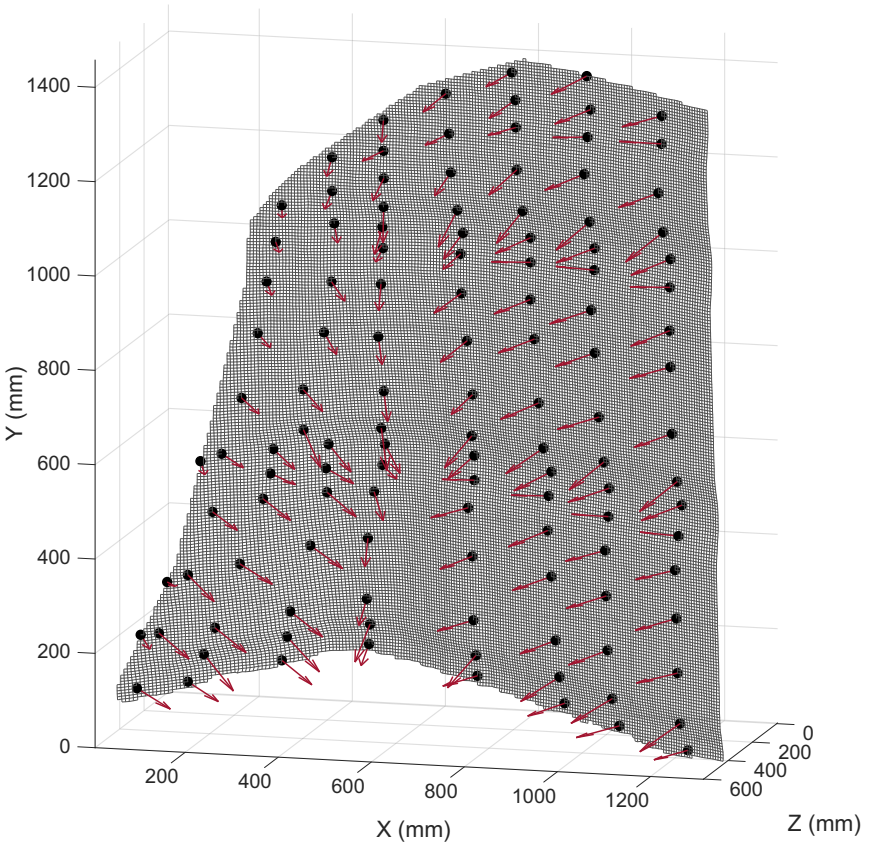

Fig. 6. Location of measurement points and directions in impact hammer test on the FP+DIC panel digitalisation.

eter as shown in Fig. 4. Therefore, full-field mode shapes in X, Y and Z direction were produced. A single value of damping, η, and natural frequency, f_n, for each mode was obtained as the mean value of the corresponding matrices. Since modal identification at the highest response points is expected to be more accurate due to higher signal-to-noise ratio, FP+DIC mode shape amplitudes of each point were employed as weight factors to increase the influence of those points on the mean value calculation, as illustrated in Fig. 4.

4. Impact hammer setup

Considering the novelty of this application, an impact hammer tests was performed as a contrasted method to validate the full-field modal analysis with FP+DIC. Specifically, 121 spatial points were evaluated. This provides an appropriate spatial resolution to avoid spatial aliasing in the present experimental work. An accelerometer was attached at the shaker excitation point to register the response of the panel to impact excitation in each point. According to Maxwell reciprocity principle, it is analogous to the FP+DIC test.

Pointwise tests in complex elements have the complicate task of precisely locating the position of the sensors, or impact points in this case. However, the information provided by FP+DIC facilitated it. The digitalisation of the panel shape was obtained consisting in the coordinates of every measurement point. Hence, impact points were associated to FP+DIC points by performing crosses in the speckle that were recognisable in the images, as shown in Fig. 5. Likewise, as the impacts were executed perpendicular to the surface, the excitation direction was easily obtained by determining the normal vector of the FP+DIC surface at the specific points (Fig. 6).

Thus, 121 FRFs were extracted from these tests. Ten samples for Welch averaging were performed per point which contained the full impact response. Eventually, the FRF frequency resolution was 0.3125 Hz in a frequency span of 1125 Hz. Then, an analogous modal analysis using the circle-fit approach was conducted to make it comparable, but now in a single direction. The later comparisons with FP+DIC mode shapes were developed by calculating the projection of the 3D information to the normal direction of the inspected points.

Please cite this article as: L. Felipe-Sesé, Á.J. Molina-Viedma, E. López-Alba et al., FP+DIC for low-cost 3D full-field experimental modal analysis in industrial components, Mechanical Systems and Signal Processing, https://doi.org/10.1016/j.ymssp.2019.04.004

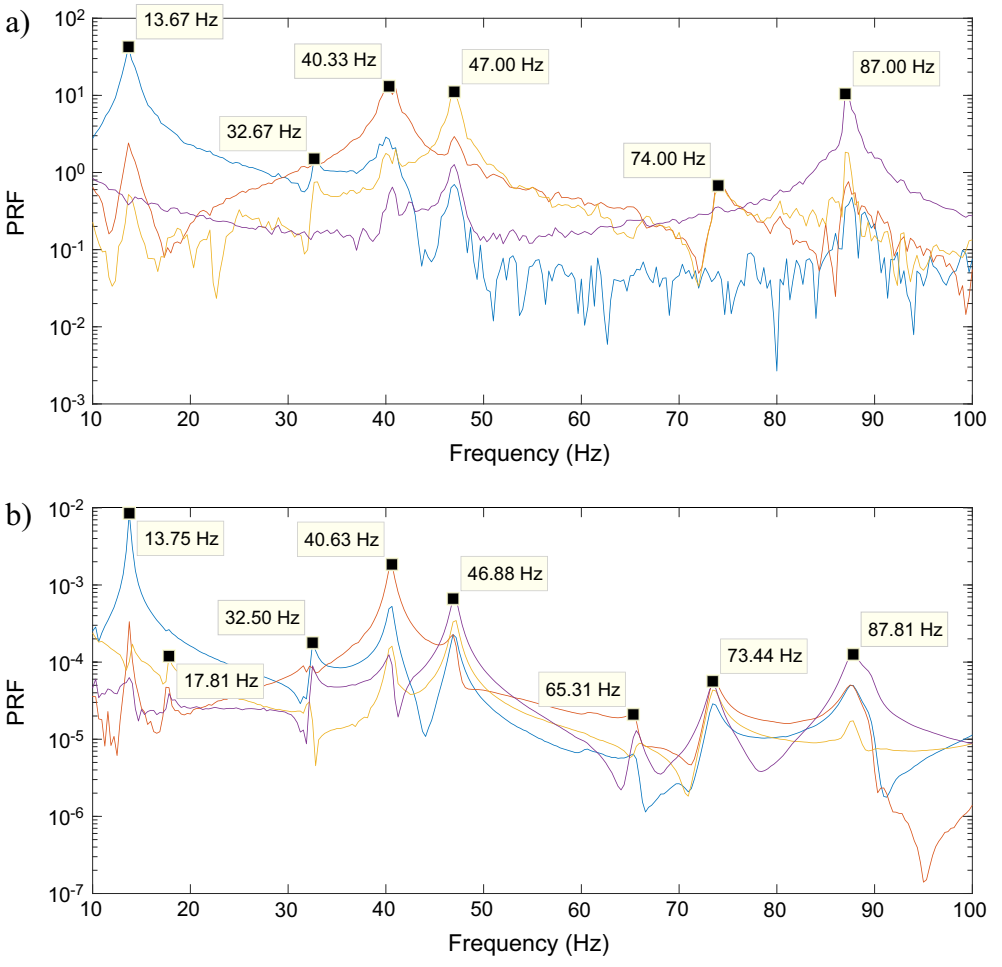

Fig. 7. Four first principal response functions from the (a) FP+DIC and (b) impact hammer tests full matrices.

Table 1
Modal parameter comparison of the six selected resonances.

		Natural frequency (Hz)	Structural damping (%)	Mode shape correlation (%)
1st mode	FP+DIC	13.82	3.68	94.59
	Impact hammer	13.86	1.99	
2nd mode	FP+DIC	32.86	3.30	89.07
	Impact hammer	32.30	1.82	
3rd mode	FP+DIC	40.54	3.46	91.28
	Impact hammer	40.51	1.59	
4th mode	FP+DIC	47.15	1.57	98.51
	Impact hammer	47.04	1.60	
5th mode	FP+DIC	74.43	2.28	66.50
	Impact hammer	73.47	1.46	
6th mode	FP+DIC	86.19	1.59	41.17
	Impact hammer	87.72	1.89	

5. Results

From the previously described procedures, full-field 3D FRFs of the panel were calculated from the single-camera FP+DIC measurements as well as the FRFs from the impact hammer tests in normal direction. This modal characterisation methodology required the identification of the resonance peaks to be analysed. Full-field techniques provided too large amounts of data to be individually inspected. Therefore, single value decomposition was employed to obtain the Principal Response Functions (PRF) [2]. This consists in multiplying the right-hand matrix by the single values matrix of the full FRFs matrix.

Please cite this article as: L. Felipe-Sesé, Á.J. Molina-Viedma, E. López-Alba et al., FP+DIC for low-cost 3D full-field experimental modal analysis in industrial components, Mechanical Systems and Signal Processing, https://doi.org/10.1016/j.ymssp.2019.04.004

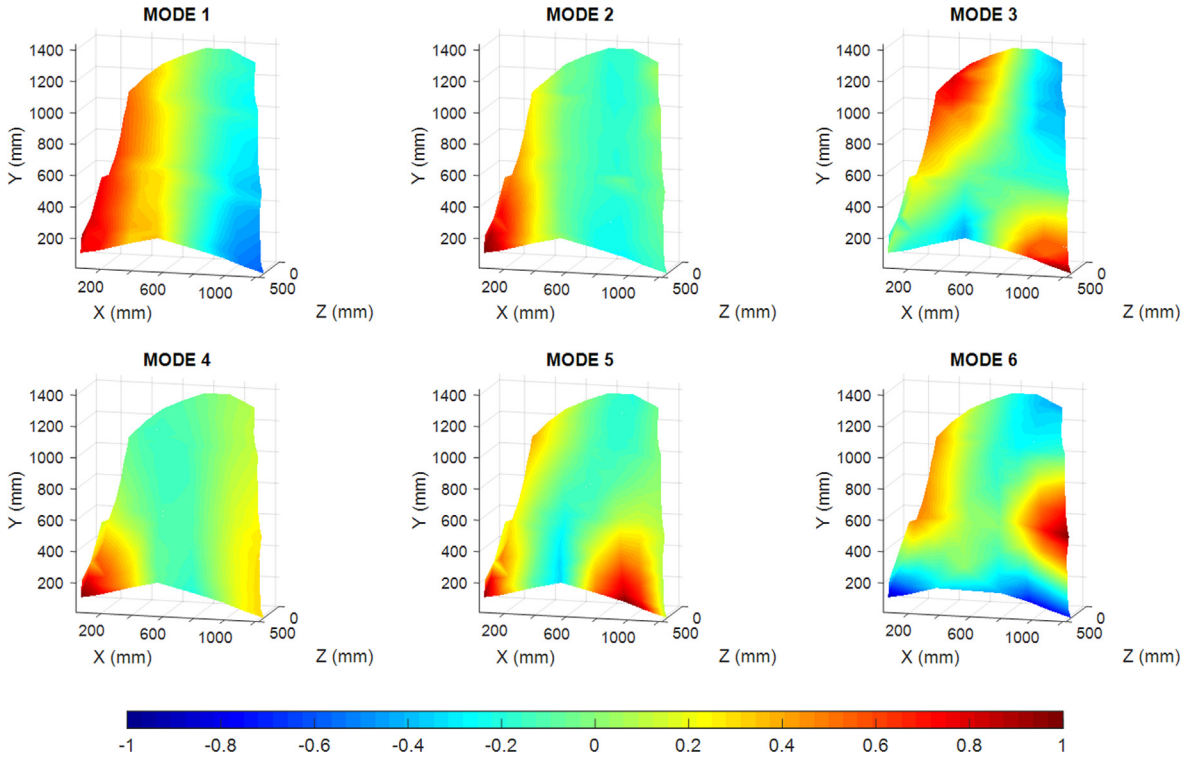

Fig. 8. Mode shapes of the composite panel in the normal direction determined from impact test measurement.

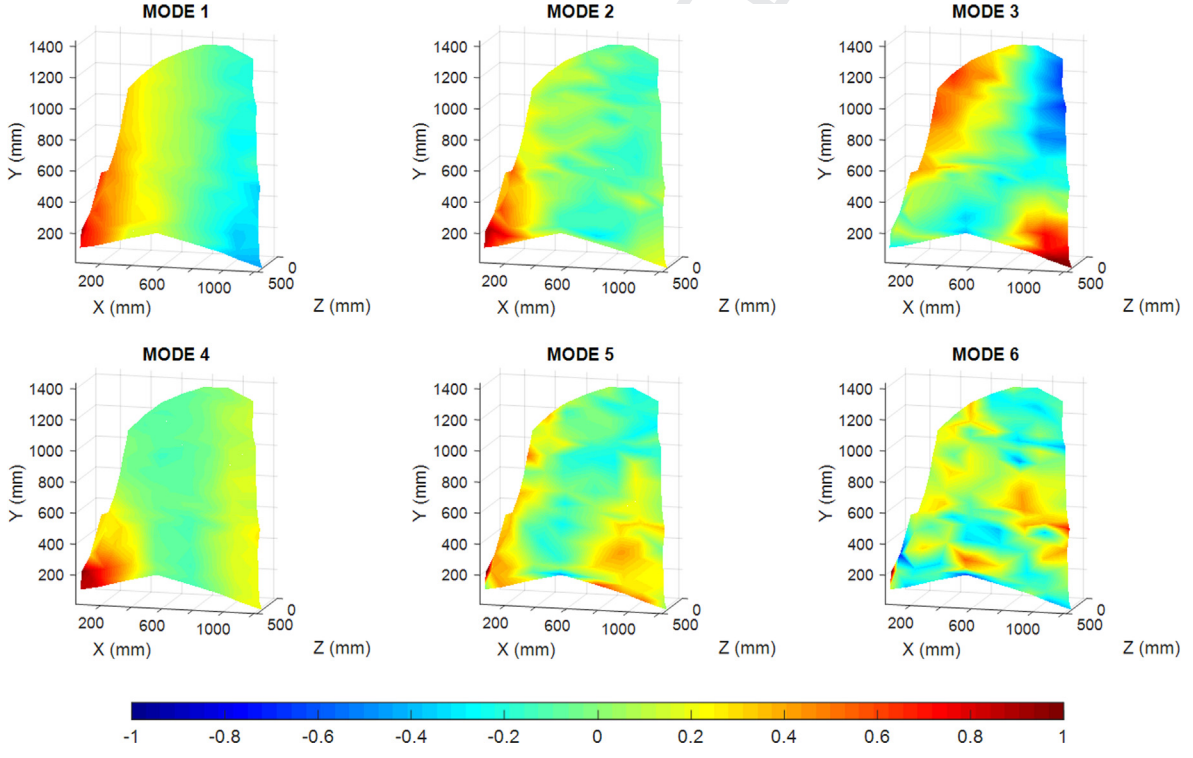

Fig. 9. Mode shapes of the composite panel in the normal direction determined from FP+DIC measurement at the impact points.

Please cite this article as: L. Felipe-Sesé, Á.J. Molina-Viedma, E. López-Alba et al., FP+DIC for low-cost 3D full-field experimental modal analysis in industrial components, Mechanical Systems and Signal Processing, https://doi.org/10.1016/j.ymssp.2019.04.004

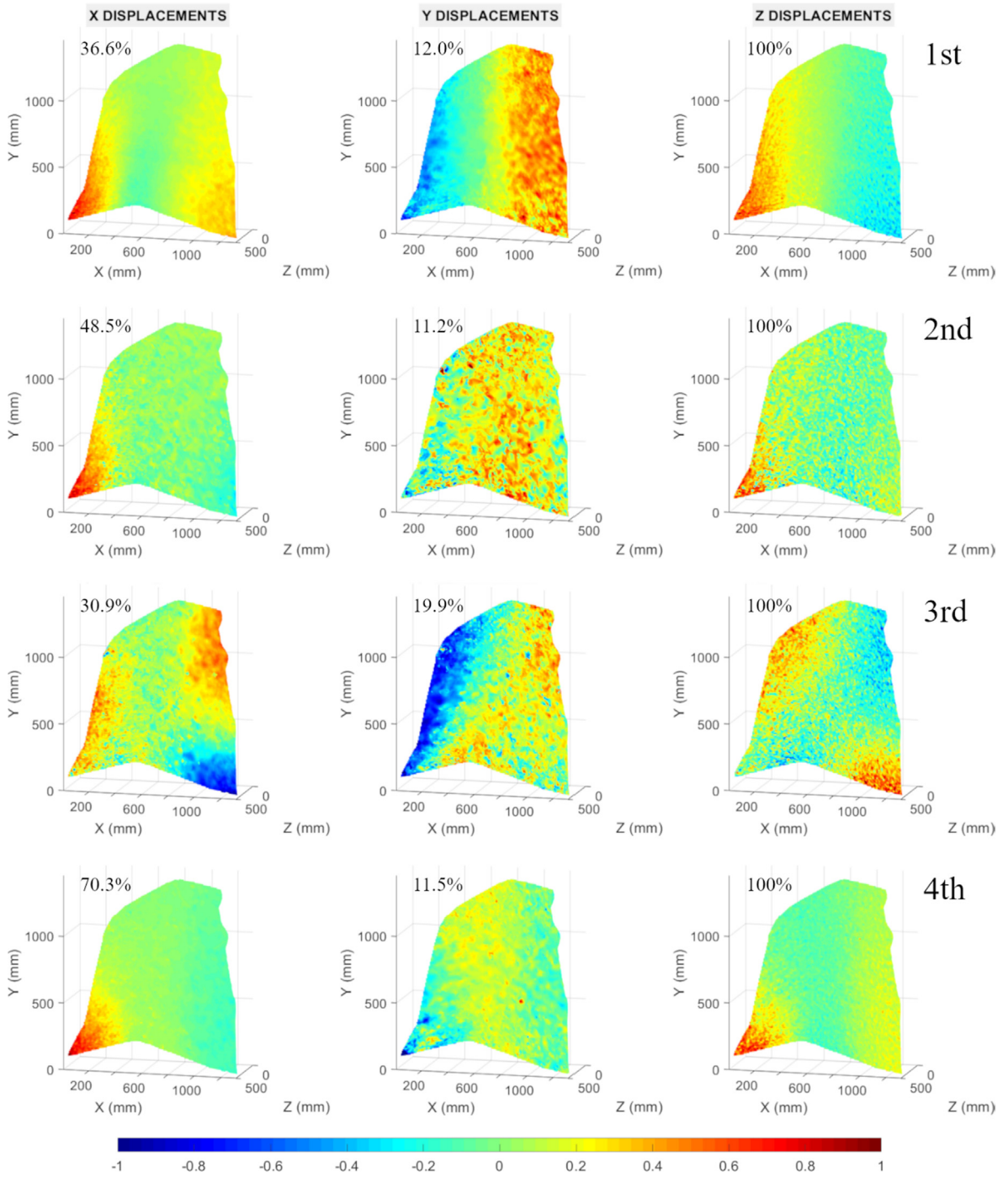

Fig. 10. First four 3D full-field mode shapes of the composite panel determined from FP+DIC measurement. Relative amplitude of each component is indicated in percentage with respect to the predominant direction.

The result is the PRFs matrix whose first columns represent a linear combination of FRFs that highlight the modes in the spectrum. The first four PRFs of FP+DIC and impact tests are depicted in Fig. 7. As can be observed, six coincident modes were found from this inspection. Additionally, the impact tests showed two exclusive modes that were too subtle to be measured by FP+DIC. These were not considered in this study.

In Table 1 the modal parameters obtained from the analysis of the six resonances using the circle-fit method are exposed. The comparison show highly stable results regarding natural frequencies for all the modes. Notable variations are found in

Please cite this article as: L. Felipe-Sesé, Á.J. Molina-Viedma, E. López-Alba et al., FP+DIC for low-cost 3D full-field experimental modal analysis in industrial components, Mechanical Systems and Signal Processing, https://doi.org/10.1016/j.ymssp.2019.04.004

structural damping, however higher uncertainty is typically present in the experimental measurement of this parameter due to higher sensitivity to boundary and ambient conditions [6,46,47]. Particularly, here it may be additionally affected by the lower signal-to-noise ratio of the technique and the shaker connection, which was not present during the impact hammer test.

However, the great attractive of the full-field information is the mode shapes. In Fig. 8 the ones extracted from impact tests are shown. Amplitudes are normalised to enable straight comparison with FP+DIC results. As previously described, this mode shapes entailed deformation in normal direction. In a traditional modal setup, even using tri-axial accelerometers, the complex shape of the panel would have made it difficult to define the location of the measurements and the orientation of the local coordinates. However, FP+DIC provided the digitalisation that allowed to make it accurately. Regarding FP+DIC, equivalent mode shapes are shown in Fig. 9 after calculating the shape in the normal direction at the same spatial points. From the comparison, evident similitudes are observed with respect to impact test mode shapes. This is confirmed by the correlation factor, given in Table 1. The most remarkable results are found for the first four modes, with a correlation over 89%. These modes are less affected by spatial noise than the other two due to the higher response in lower frequencies. The full-field shapes of these four modes are presented in Fig. 10 in each of the three directions. They were also normalised and the relative amplitudes in percentage are indicated with respect to the most predominant deformation direction. As a consequence of the plate behaviour of the panel, out-of-plane Z direction shows the highest amplitudes whereas Y deformation is the least relevant. Despite the low correlation factor in fifth and sixth modes, similitudes can be noticed. Moreover, damping ratio and, especially, natural frequencies are in agreement with impact test results. Therefore, the modal identification for these higher order modes was able to give a first approach that can be completed or assessed through additional analysis with higher sensitivity pointwise transducers or laser vibrometry.

6. Conclusions

In this study, the integration of FP and DIC has been proposed as a low-cost alternative to HS 3D-DIC for experimental modal analysis. Considering the different alternative methodologies and techniques that employ a single camera, this is actually the first study that performs a complete modal analysis using well-established procedures and full-field 3D information with a single-camera technique. Moreover, this work has been performed in an aeronautical panel with noteworthy 3D behaviour what shows the capabilities of the technique for real industrial components beyond typical flat, benchmark examples. Circle-fit approach was employed for modal identification and the results were validated using a standard impact hammer test. As a result, accurate modal parameters were obtained for different resonances, especially highlighting 3D mode shapes. Typical limitations in higher order modes were found according to the sensitivity of such non-interferometric techniques. At the same time, the study showed the improvements over a classical pointwise configuration such as location and orientation of measurement points in non-flat surfaces. In conclusion, this technique has proved to be suitable to perform 3D modal characterisations in a full-field manner.

References

[1] J. Baqersad, P. Poozesh, C. Niezrecki, P. Avitabile, Photogrammetry and optical methods in structural dynamics – a review, Mech. Syst. Signal Process. 86 (2017) 17–34, https://doi.org/10.1016/j.ymssp.2016.02.011.
[2] D.J. Ewins, Modal Testing: Theory, Practice, and Application, 2nd ed., Research Studies Press LTD, Baldock, Hertfordshire, England, 2000.
[3] K.G. McConnell, P.S. Varoto, Vibration Testing: Theory and Practice, 2nd ed., Wiley, 2008.
[4] M.N. Helfrick, C. Niezrecki, P. Avitabile, T. Schmidt, 3D digital image correlation methods for full-field vibration measurement, Mech. Syst. Signal Process. 25 (2011) 917–927, https://doi.org/10.1016/j.ymssp.2010.08.013.
[5] C. Warren, C. Niezrecki, P. Avitabile, P. Pingle, Comparison of FRF measurements and mode shapes determined using optically image based, laser, and accelerometer measurements, Mech. Syst. Signal Process. 25 (2011) 2191–2202, https://doi.org/10.1016/j.ymssp.2011.01.018.
[6] P.L. Reu, D.P. Rohe, L.D. Jacobs, Comparison of DIC and LDV for practical vibration and modal measurements, Mech. Syst. Signal Process. 86 (2017) 2–16, https://doi.org/10.1016/j.ymssp.2016.02.006.
[7] H. Schreier, J.-J. Orteu, M.A. Sutton, in: Image Correlation for Shape, Motion and Deformation Measurements, Springer US, Boston, MA, MA, 2009, https://doi.org/10.1007/978-0-387-78747-3.
[8] T. Siebert, R. Wood, K. Splitthof, High speed image correlation for vibration analysis, J. Phys. Conf. Ser. 7th Int. Conf. Mod. Pract. Stress Vib. Anal. 181 (2009), https://doi.org/10.1088/1742-6596/181/1/012064 012064.
[9] W. Wang, J.E. Mottershead, A. Ihle, T. Siebert, H.R. Schubach, Finite element model updating from full-field vibration measurement using digital image correlation, J. Sound Vib. 330 (2011) 1599–1620, https://doi.org/10.1016/j.jsv.2010.10.036.
[10] D.A. Ehrhardt, M.S. Allen, S. Yang, T.J. Beberniss, Full-field linear and nonlinear measurements using Continuous-Scan Laser Doppler Vibrometry and high speed Three-Dimensional Digital Image Correlation, Mech. Syst. Signal Process. 86 (2017) 82–97, https://doi.org/10.1016/j.ymssp.2015.12.003.
[11] A.J. Molina-Viedma, L. Felipe-Sesé, E. López-Alba, F.A. Díaz, 3D mode shapes characterisation using phase-based motion magnification in large structures using stereoscopic DIC, Mech. Syst. Signal Process. 108 (2018) 140–155, https://doi.org/10.1016/j.ymssp.2018.02.006.
[12] J. Baqersad, J. Carr, T. Lundstrom, C. Niezrecki, P. Avitabile, M. Slattery, Dynamic characteristics of a wind turbine blade using 3D digital image correlation, in: T. Kundu (Ed.), Proc. SPIE, 2012, p. 83482I, https://doi.org/10.1117/12.915377.
[13] Á. Molina-Viedma, E. López-Alba, L. Felipe-Sesé, F. Díaz, J. Rodríguez-Ahlquist, M. Iglesias-Vallejo, Modal Parameters Evaluation in a Full-Scale Aircraft Demonstrator under Different Environmental Conditions Using HS 3D-DIC, Materials (Basel) 11 (2018) 230, https://doi.org/10.3390/ma11020230.
[14] F. Trebuña, M. Hagara, Experimental modal analysis performed by high-speed digital image correlation system, Measurement. 50 (2014) 78–85, https://doi.org/10.1016/j.measurement.2013.12.038.
[15] R. Huňady, M. Hagara, A new procedure of modal parameter estimation for high-speed digital image correlation, Mech. Syst. Signal Process. 93 (2017) 66–79, https://doi.org/10.1016/j.ymssp.2017.02.010.
[16] Á.J. Molina-Viedma, E. López-Alba, L. Felipe-Sesé, F.A. Díaz, Full-field modal analysis during base motion excitation using high-speed 3D digital image correlation, Meas. Sci. Technol. 28 (2017), https://doi.org/10.1088/1361-6501/aa7d87 105402.

Please cite this article as: L. Felipe-Sesé, Á.J. Molina-Viedma, E. López-Alba et al., FP+DIC for low-cost 3D full-field experimental modal analysis in industrial components, Mechanical Systems and Signal Processing, https://doi.org/10.1016/j.ymssp.2019.04.004

[17] N.S. Ha, H.M. Vang, N.S. Goo, Modal analysis using digital image correlation technique: an application to artificial wing mimicking beetle's hind wing, Exp. Mech. (2015) 989–998, https://doi.org/10.1007/s11340-015-9987-2.
[18] W. Wang, J.E. Mottershead, T. Siebert, A. Pipino, Frequency response functions of shape features from full-field vibration measurements using digital image correlation, Mech. Syst. Signal Process. 28 (2012) 333–347, https://doi.org/10.1016/j.ymssp.2011.11.023.
[19] Á. Molina-Viedma, E. López-Alba, L. Felipe-Sesé, F. Díaz, Modal identification in an automotive multi-component system using HS 3D-DIC, Materials (Basel) 11 (2018) 241, https://doi.org/10.3390/ma11020241.
[20] B. Pan, L. Yu, Q. Zhang, Review of single-camera stereo-digital image correlation techniques for full-field 3D shape and deformation measurement, Sci. China Technol. Sci. 61 (2018) 2–20, https://doi.org/10.1007/s11431-017-9090-x.
[21] B. Pan, Q. Wang, Single-camera microscopic stereo digital image correlation using a diffraction grating, Opt. Express. (2013), https://doi.org/10.1364/OE.21.025056.
[22] L.F. Wu, J.G. Zhu, H.M. Xie, Q. Zhang, an accurate method for shape retrieval and displacement measurement using bi-prism-based single lens 3D digital image correlation, Exp. Mech. (2016), https://doi.org/10.1007/s11340-016-0193-7.
[23] E. López-Alba, L. Felipe-Sesé, S. Schmeer, F.A. Díaz, Optical low-cost and portable arrangement for full field 3D displacement measurement using a single camera, Meas. Sci. Technol. 27 (2016), https://doi.org/10.1088/0957-0233/27/11/115901 115901.
[24] L. Yu, B. Pan, Single-camera high-speed stereo-digital image correlation for full-field vibration measurement, Mech. Syst. Signal Process. 94 (2017) 374–383, https://doi.org/10.1016/j.ymssp.2017.03.008.
[25] C. Mares, B. Barrientos, A. Blanco, Measurement of transient deformation by color encoding, Opt. Express. 19 (2011), https://doi.org/10.1364/OE.19.025712.
[26] B. Barrientos, M. Cerca, J. García-Márquez, C. Hernández-Bernal, Three-dimensional displacement fields measured in a deforming granular-media surface by combined fringe projection and speckle photography, J. Opt. A Pure Appl. Opt. 10 (2008), https://doi.org/10.1088/1464-4258/10/10/104027 104027.
[27] C.J. Tay, C. Quan, T. Wu, Y.H. Huang, Integrated method for 3-D rigid-body displacement measurement using fringe projection, Opt. Eng. 43 (2004) 1152, https://doi.org/10.1117/1.1687728.
[28] H. Shi, H. Ji, G. Yang, X. He, Shape and deformation measurement system by combining fringe projection and digital image correlation, Opt. Lasers Eng. 51 (2013) 47–53, https://doi.org/10.1016/j.optlaseng.2012.07.020.
[29] C.J. Tay, C. Quan, Y.H. Huang, Y. Fu, Digital image correlation for whole field out-of-plane displacement measurement using a single camera, Opt. Commun. 251 (2005) 23–36, https://doi.org/10.1016/j.optcom.2005.02.070.
[30] C. Quan, C.J. Tay, Y.H. Huang, 3-D deformation measurement using fringe projection and digital image correlation, Opt. – Int. J. Light Electron Opt. 115 (2004) 164–168, https://doi.org/10.1016/S0030-4026(08)70004-4.
[31] P. Siegmann, V. Álvarez-Fernández, F. Díaz-Garrido, E.A. Patterson, A simultaneous in- and out-of-plane displacement measurement method, Opt. Lett. 36 (2011) 10, https://doi.org/10.1364/OL.36.000010.
[32] T.N. Nguyen, J.M. Huntley, R.L. Burguete, C.R. Coggrave, Multiple-view shape and deformation measurement by combining fringe projection and digital image correlation, Strain 48 (2012) 256–266, https://doi.org/10.1111/j.1475-1305.2011.00819.x.
[33] L. Felipe-Sesé, P. Siegmann, F.A. Díaz, E.A. Patterson, Simultaneous in-and-out-of-plane displacement measurements using fringe projection and digital image correlation, Opt. Lasers Eng. 52 (2014) 66–74, https://doi.org/10.1016/j.optlaseng.2013.07.025.
[34] L. Felipe-Sesé, P. Siegmann, F.A. Díaz, E.A. Patterson, Integrating fringe projection and digital image correlation for high-quality measurements of shape changes, Opt. Eng. 53 (2014), https://doi.org/10.1117/1.OE.53.4.044106 044106.
[35] R. Ramanath, W.E. Snyder, G.L. Bilbro, W.A. Sander, Demosaicking methods for Bayer color arrays, J. Electron. Imaging. 11 (2002) 306, https://doi.org/10.1117/1.1484495.
[36] L. Felipe-Sesé, F.A. Díaz, Damage methodology approach on a composite panel based on a combination of Fringe Projection and 2D Digital Image Correlation, Mech. Syst. Signal Process. 101 (2018) 467–479, https://doi.org/10.1016/j.ymssp.2017.09.002.
[37] L. Felipe-Sesé, F.A. Diaz-Garrido, E.A. Patterson, Exploiting measurement-based validation for a high-fidelity model of dynamic indentation of a hyperelastic material, Int. J. Solids Struct. 97–98 (2016) 520–529, https://doi.org/10.1016/j.ijsolstr.2016.06.036.
[38] M. Takeda, K. Mutoh, Fourier transform profilometry for the automatic measurement of 3-D object shapes, Appl. Opt. 22 (1983) 3977, https://doi.org/10.1364/AO.22.003977.
[39] B. Pan, K. Qian, H. Xie, A. Asundi, Two-dimensional digital image correlation for in-plane displacement and strain measurement : a review, Meas. Sci. Technol. 20 (2009) 1–17, https://doi.org/10.1088/0957-0233/20/6/062001.
[40] M. Sutton, W. Wolters, W. Peters, W. Ranson, S. McNeill, Determination of displacements using an improved digital correlation method, Image Vis. Comput. 1 (1983) 133–139, https://doi.org/10.1016/0262-8856(83)90064-1.
[41] P. Siegmann, L. Felipe-Sese, F. Diaz-Garrido, Improved 3D displacement measurements method and calibration of a combined fringe projection and 2D-DIC system, Opt. Lasers Eng. 88 (2017) 255–264, https://doi.org/10.1016/j.optlaseng.2016.08.014.
[42] L. Felipe-Sesé, Á.J. Molina-Viedma, E. López-Alba, F.A. Díaz, RGB colour encoding improvement for three-dimensional shapes and displacement measurement using the integration of fringe projection and digital image correlation, Sensors (Switzerland) 18 (2018), https://doi.org/10.3390/s18093130.
[43] M. Takeda, H. Ina, S. Kobayashi, Fourier-transform method of fringe-pattern analysis for computer-based topography and interferometry, J. Opt. Soc. Am. 72 (1982) 156, https://doi.org/10.1364/JOSA.72.000156.
[44] D. Ghiglia, M. Pritt, Two-dimensional phase unwrapping: theory, algorithms, and software, 1998. doi:10.1177/004057368303900411.
[45] P.D. Welch, The use of fast Fourier transform for the estimation of power spectra: a method based on time averaging over short, modified Periodograms, IEEE Trans. Audio Electroacoust. 15 (1967) 70–73, https://doi.org/10.1109/TAU.1967.1161901.
[46] B.J. Lazan, Damping of materials and members in structural mechanics, 1st ed., Pergamon Press, Oxford (NY, USA), 1968.
[47] T.J. Beberniss, D.A. Ehrhardt, High-speed 3D digital image correlation vibration measurement: recent advancements and noted limitations, Mech. Syst. Signal Process. 86 (2017) 35–48, https://doi.org/10.1016/j.ymssp.2016.04.014.

Please cite this article as: L. Felipe-Sesé, Á.J. Molina-Viedma, E. López-Alba et al., FP+DIC for low-cost 3D full-field experimental modal analysis in industrial components, Mechanical Systems and Signal Processing, https://doi.org/10.1016/j.ymssp.2019.04.004